Supplementary materials

Synthesis and antioxidant activity of new catechol thioethers with the methylene linker

Ivan V. Smolyaninov[*,1], Daria A. Burmistrova[1], Maxim V. Arsenyev[2], Maria A. Polovinkina[3], Nadezhda P. Pomortseva[1], Georgy K. Fukin[2], Andrey I. Poddel'sky[*,2], Nadezhda T. Berberova[1]

[1] Department of Chemistry, Astrakhan State Technical University, 16 Tatisheva str., Astrakhan, 414056, Russia

[2] G.A. Razuvaev Institute of Organometallic Chemistry, Russian Academy of Sciences, 49 Tropinina str., 603137, Nizhny Novgorod, Russia

[3] Toxicology research group of Southern Scientific Centre of Russian Academy of Science, 41 Chekhova str., Rostov-on-Don, 344006, Russia

Content:

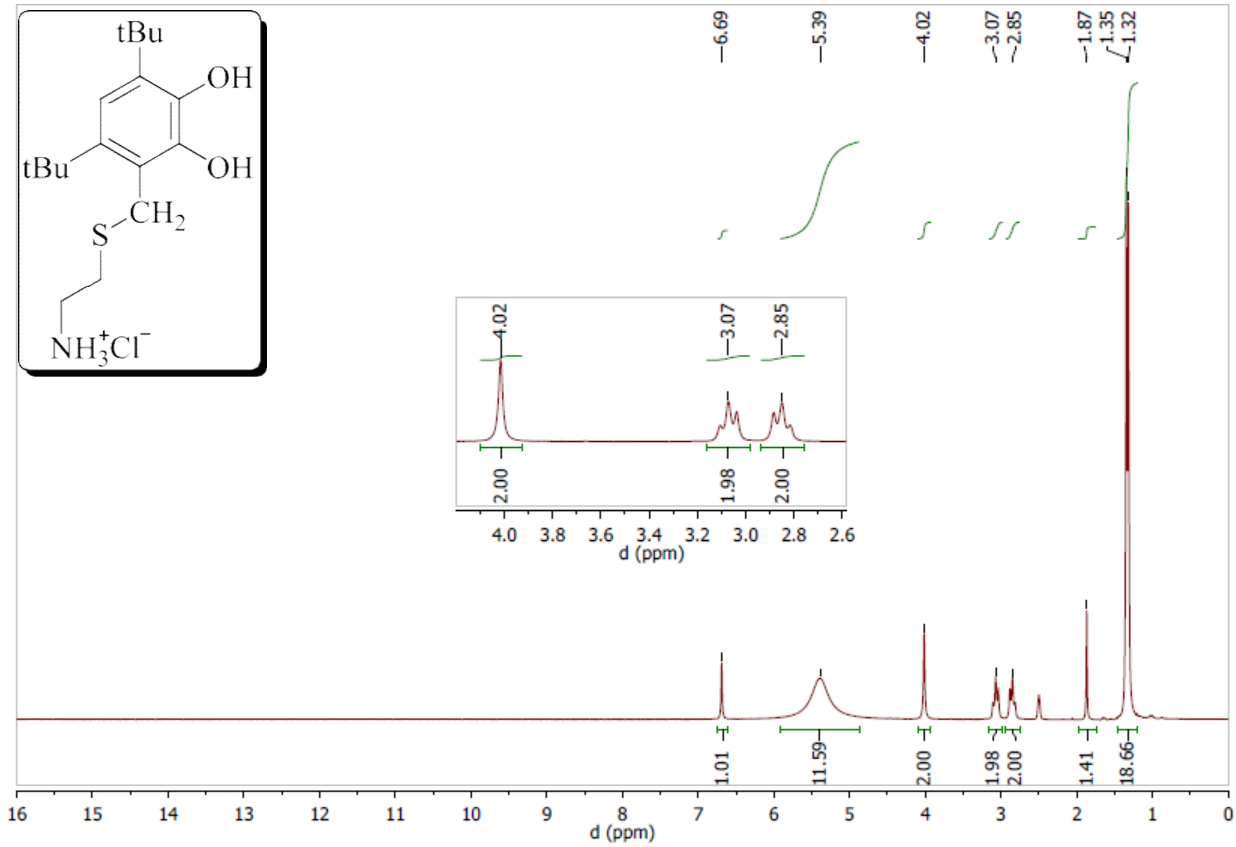

Figure S1. The ^{1}H NMR spectrum of **1** (200 MHz, DMSO-d_6).

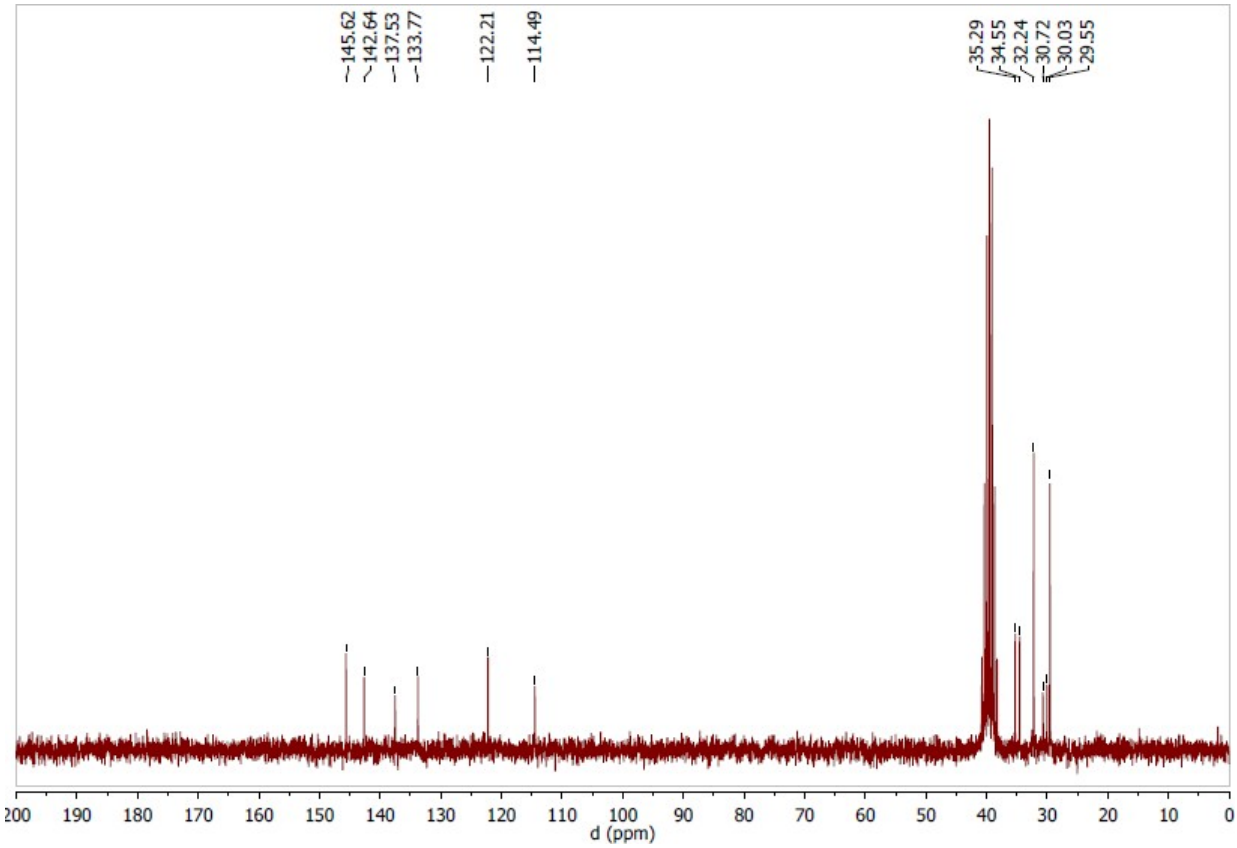

Figure S2. The ^{13}C{^{1}H} NMR spectrum of **1** (50 MHz, DMSO-d_6).

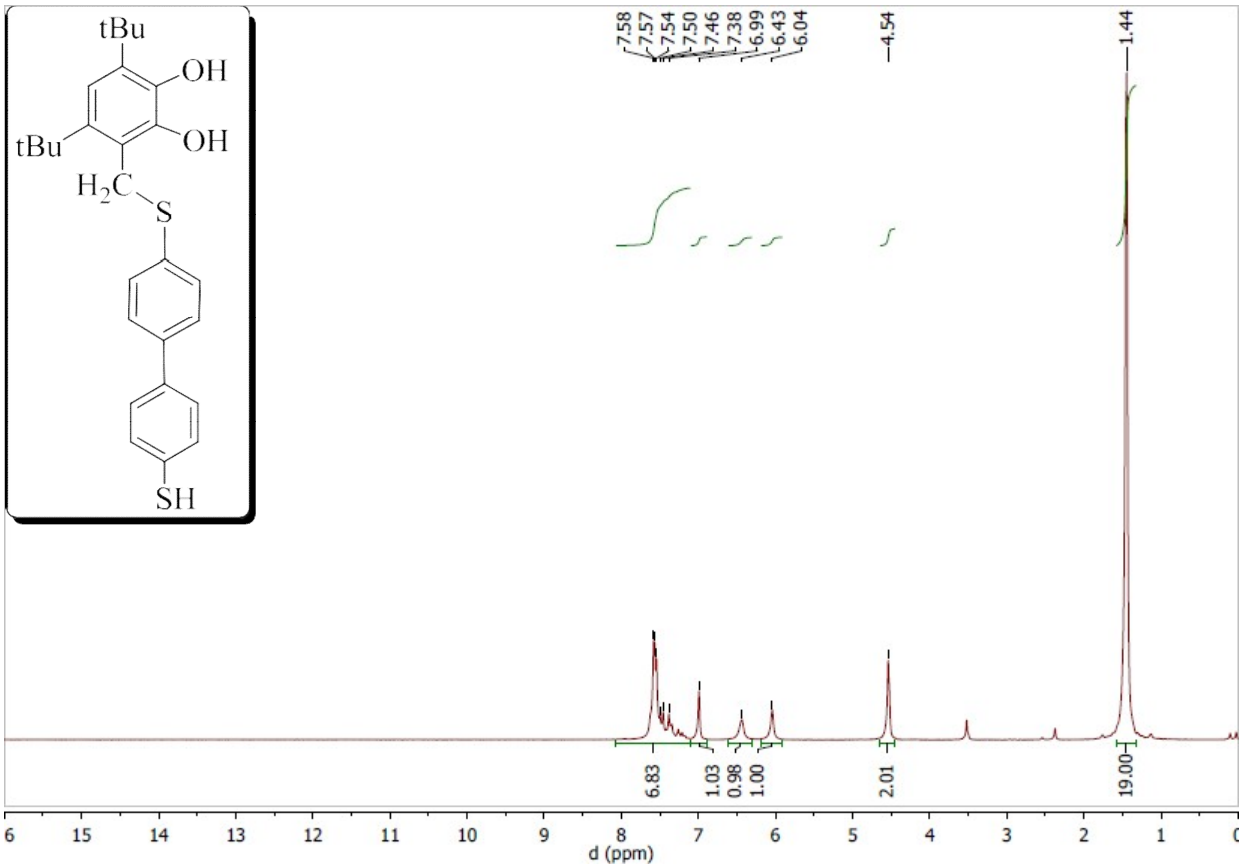

Figure S3. The ^{1}H NMR spectrum of **2** (200 MHz, $CDCl_3$).

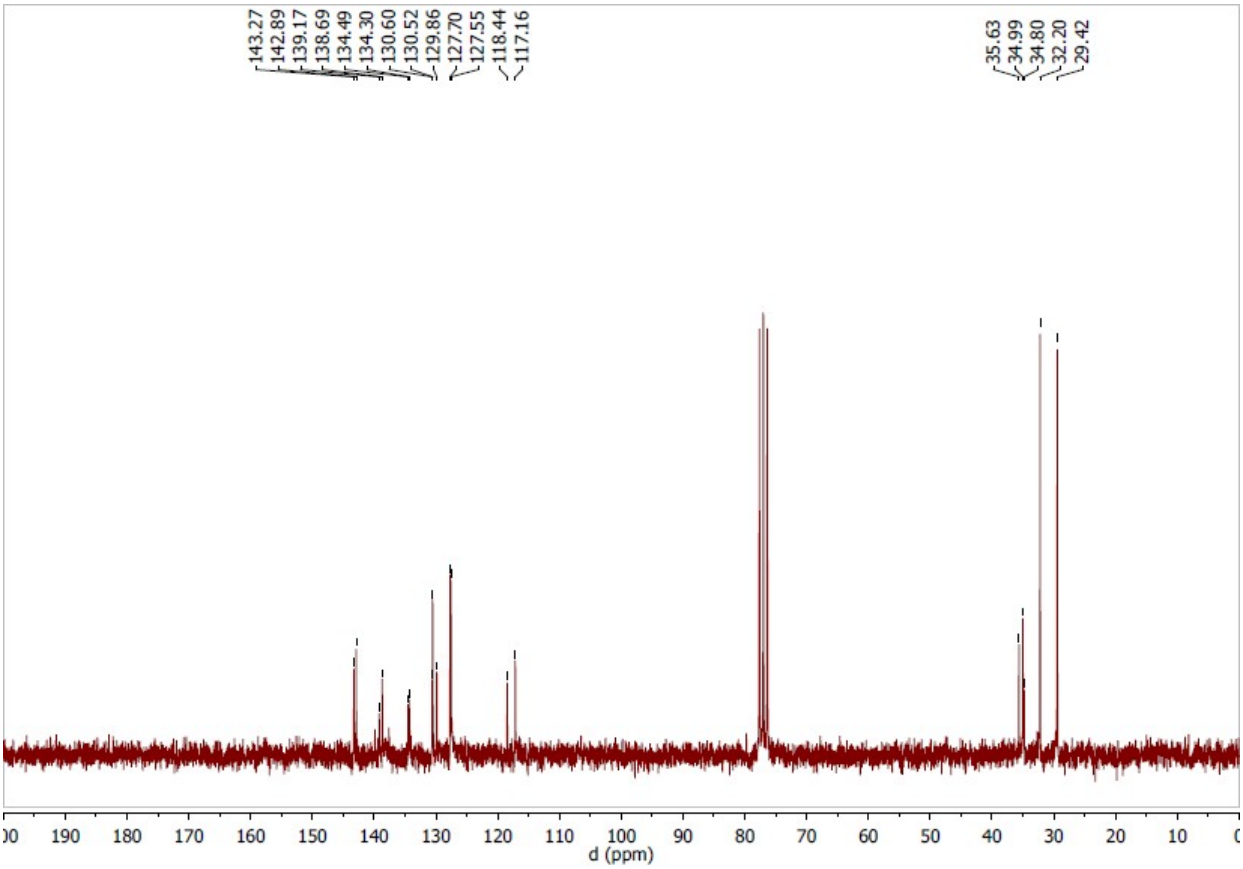

Figure S4. The $^{13}C\{^{1}H\}$ NMR spectrum of **2** (50 MHz, $CDCl_3$).

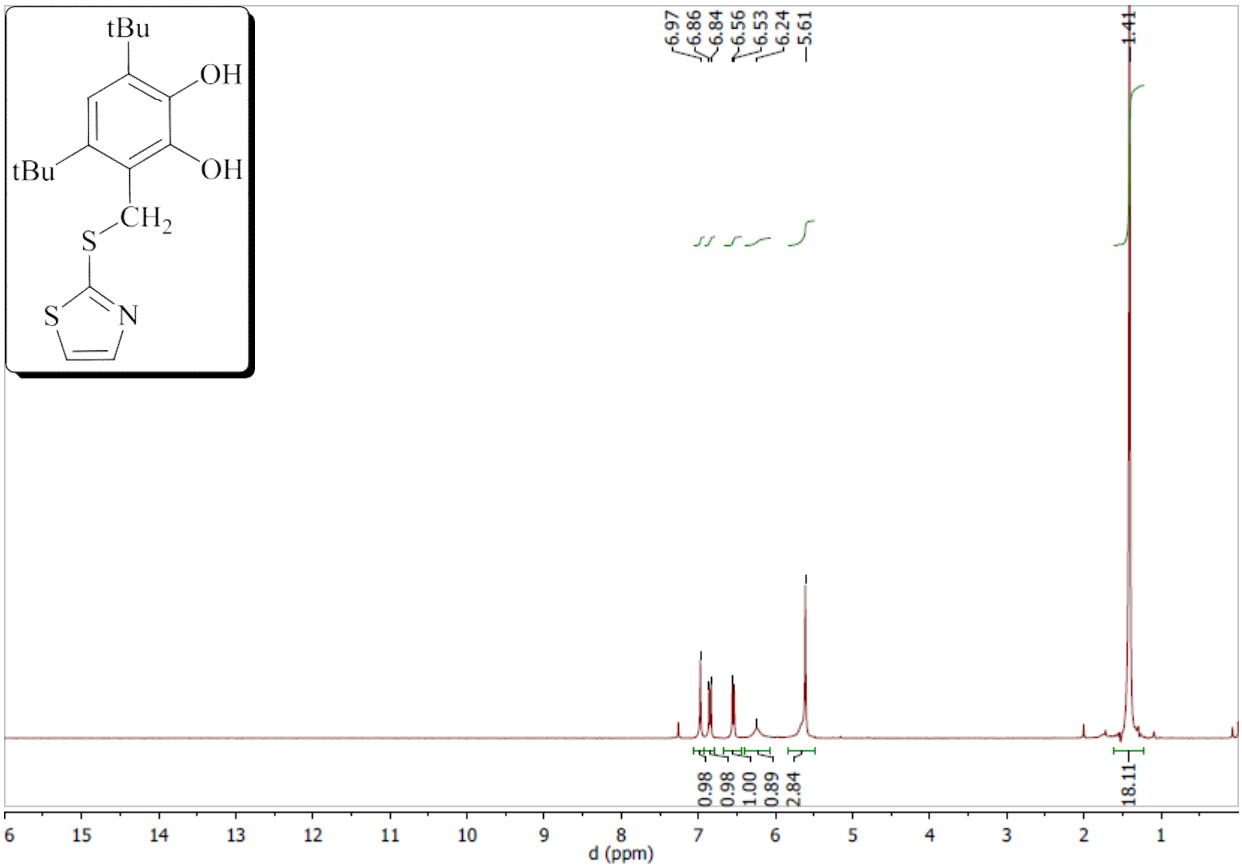

Figure S5. The ^{1}H NMR spectrum of **4** (200 MHz, $CDCl_3$).

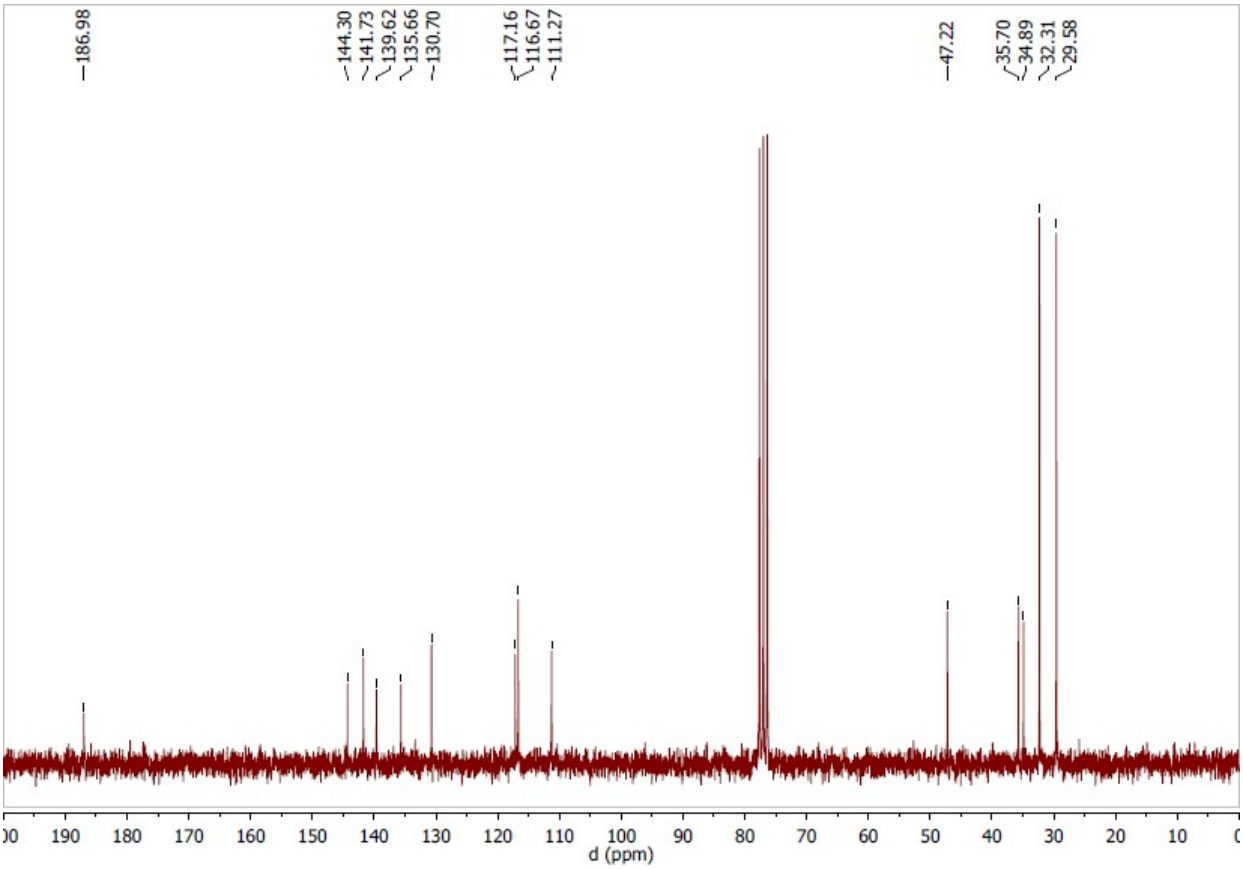

Figure S6. The $^{13}C\{^{1}H\}$ NMR spectrum of **4** (50 MHz, $CDCl_3$).

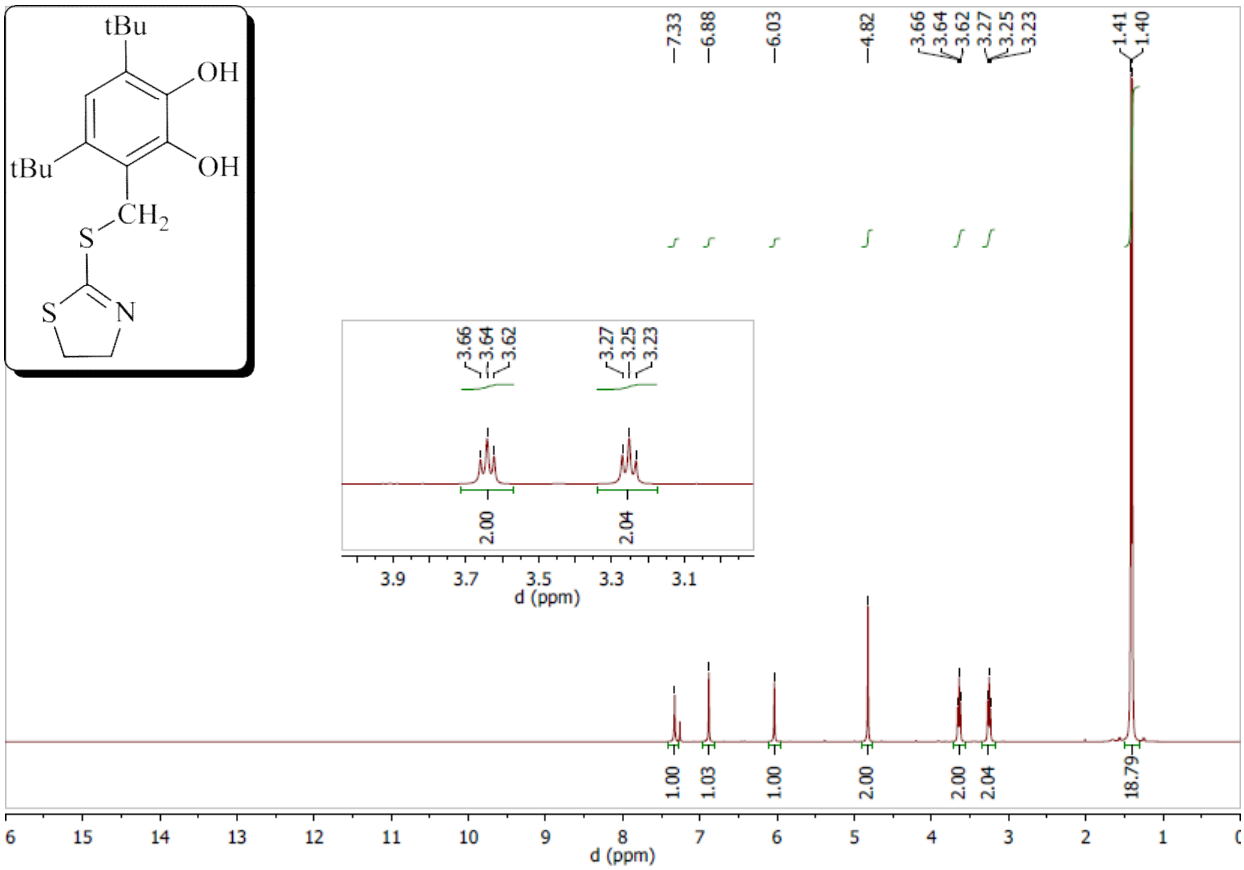

Figure S7. The ^{1}H NM R spectrum of **5** (400 MHz, $CDCl_3$).

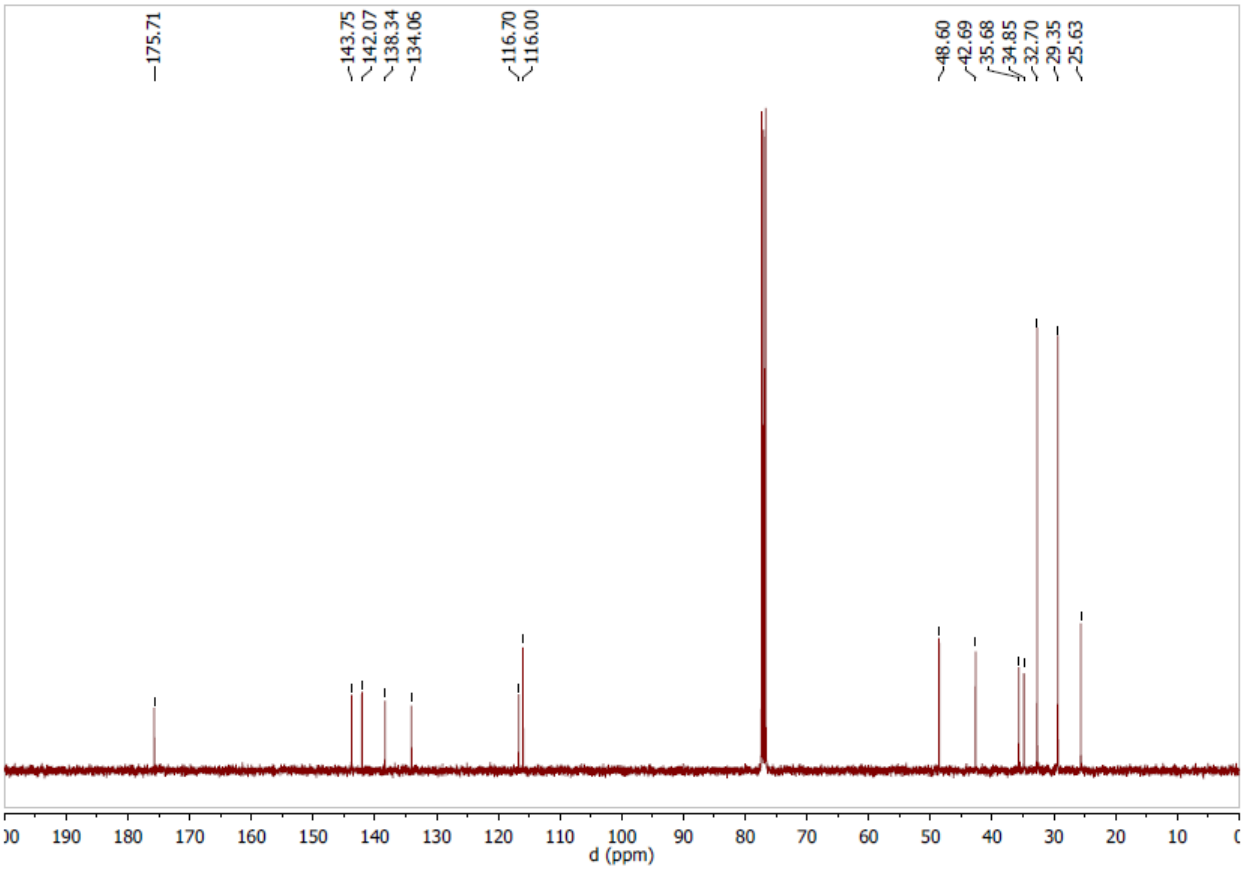

Figure S8. The $^{13}C\{^{1}H\}$ NMR spectrum of **5** (100 MHz, $CDCl_3$).

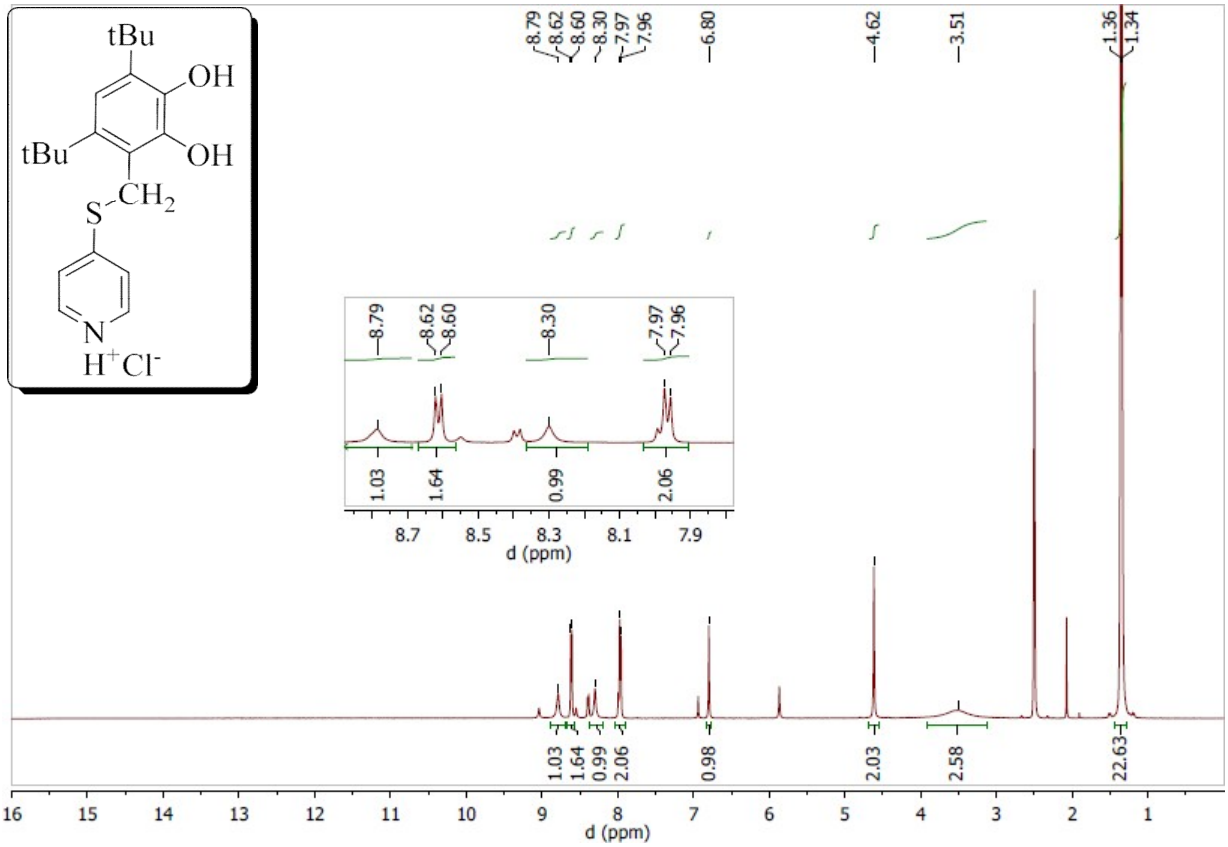

Figure S9. The ^{1}H NMR spectrum of **6** (200 MHz, DMSO-d_6).

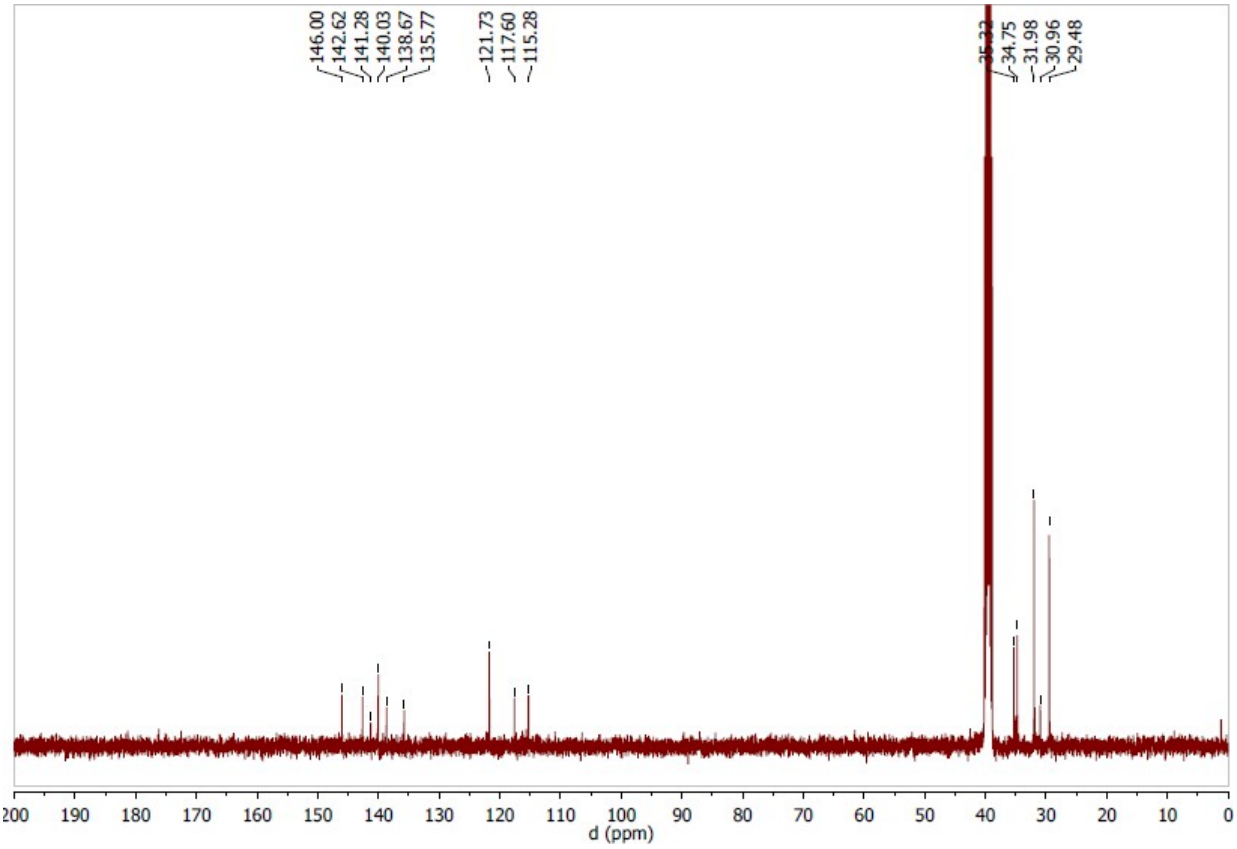

Figure S10. The $^{13}C\{^{1}H\}$ NMR spectrum of **6** (50 MHz, DMSO-d_6).

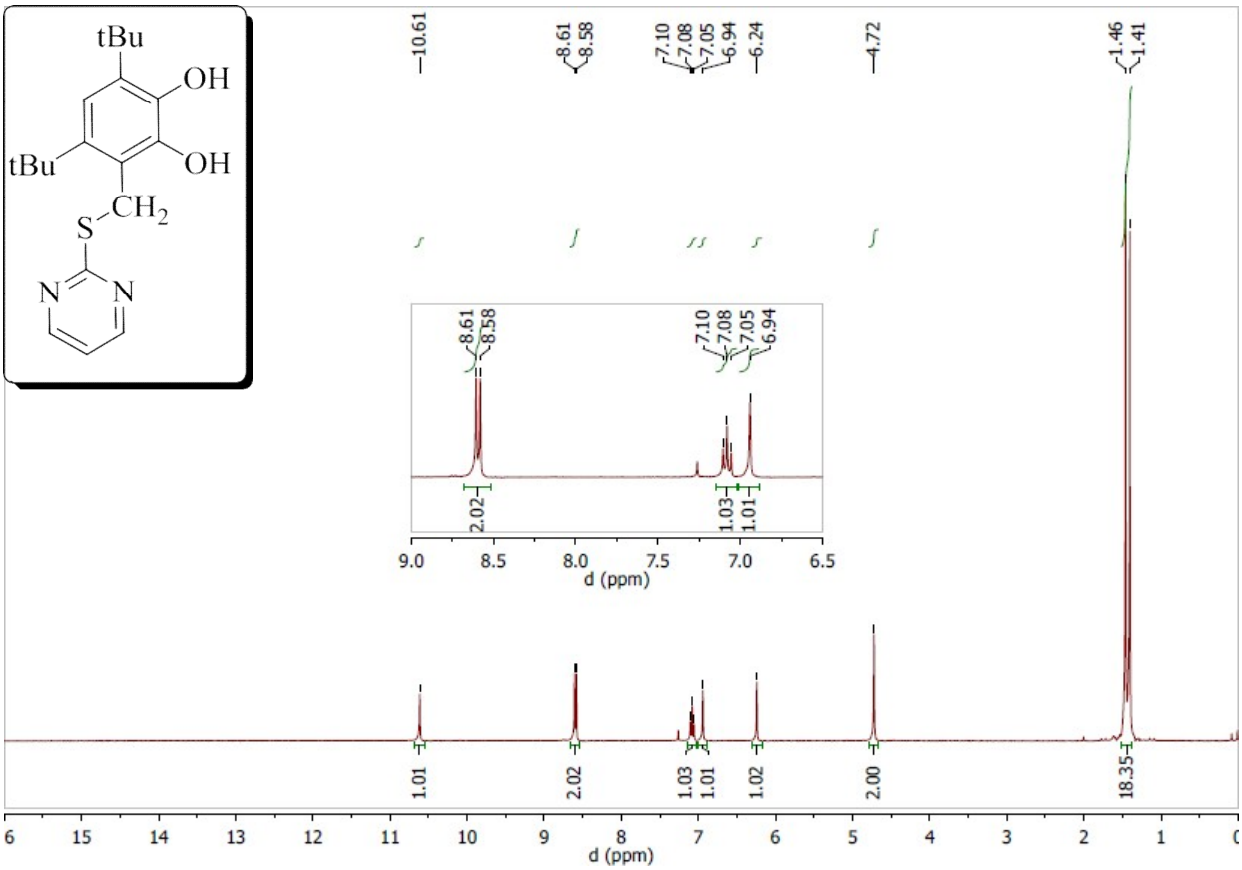

Figure S11. The ^{1}H NMR spectrum of **7** (200 MHz, $CDCl_3$).

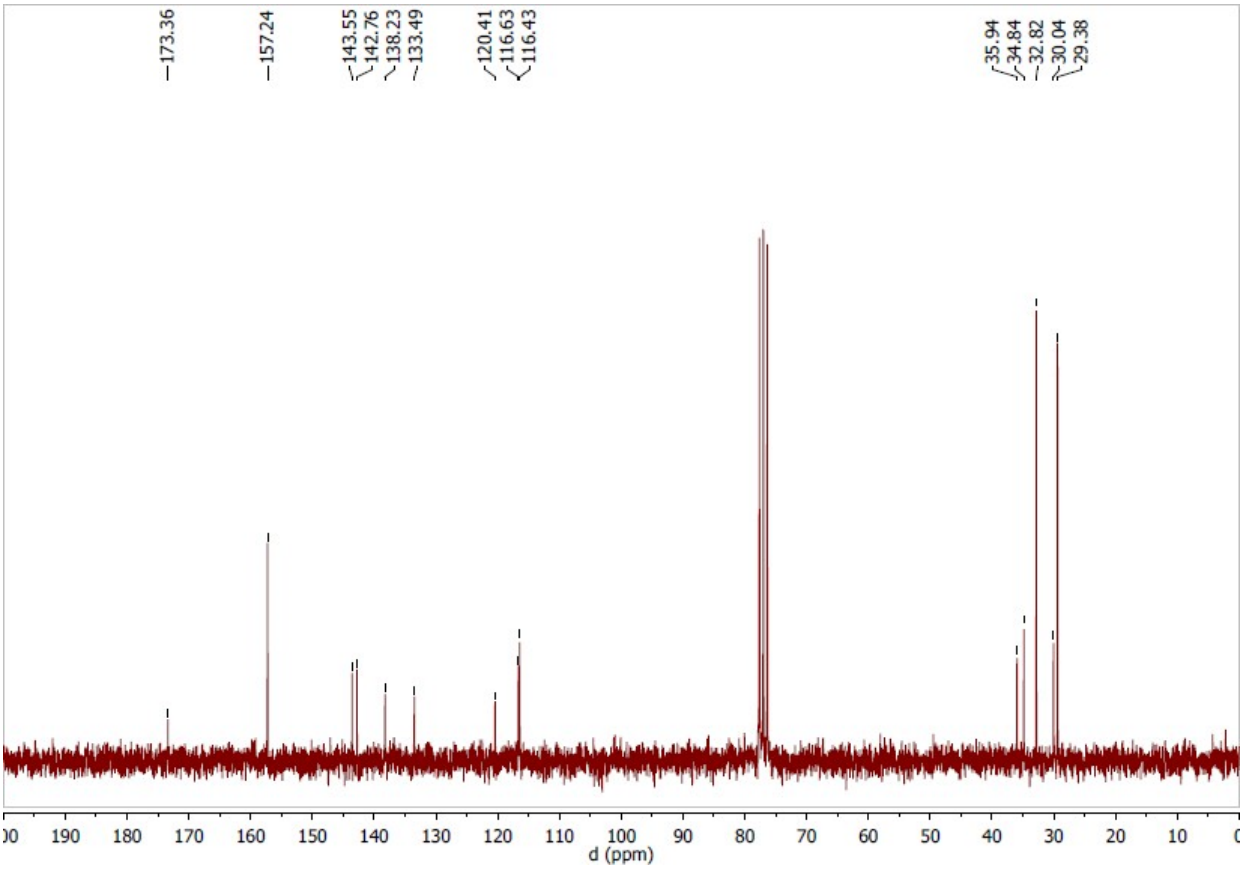

Figure S12. The $^{13}C\{^{1}H\}$ NMR spectrum of **7** (50 MHz, $CDCl_3$).

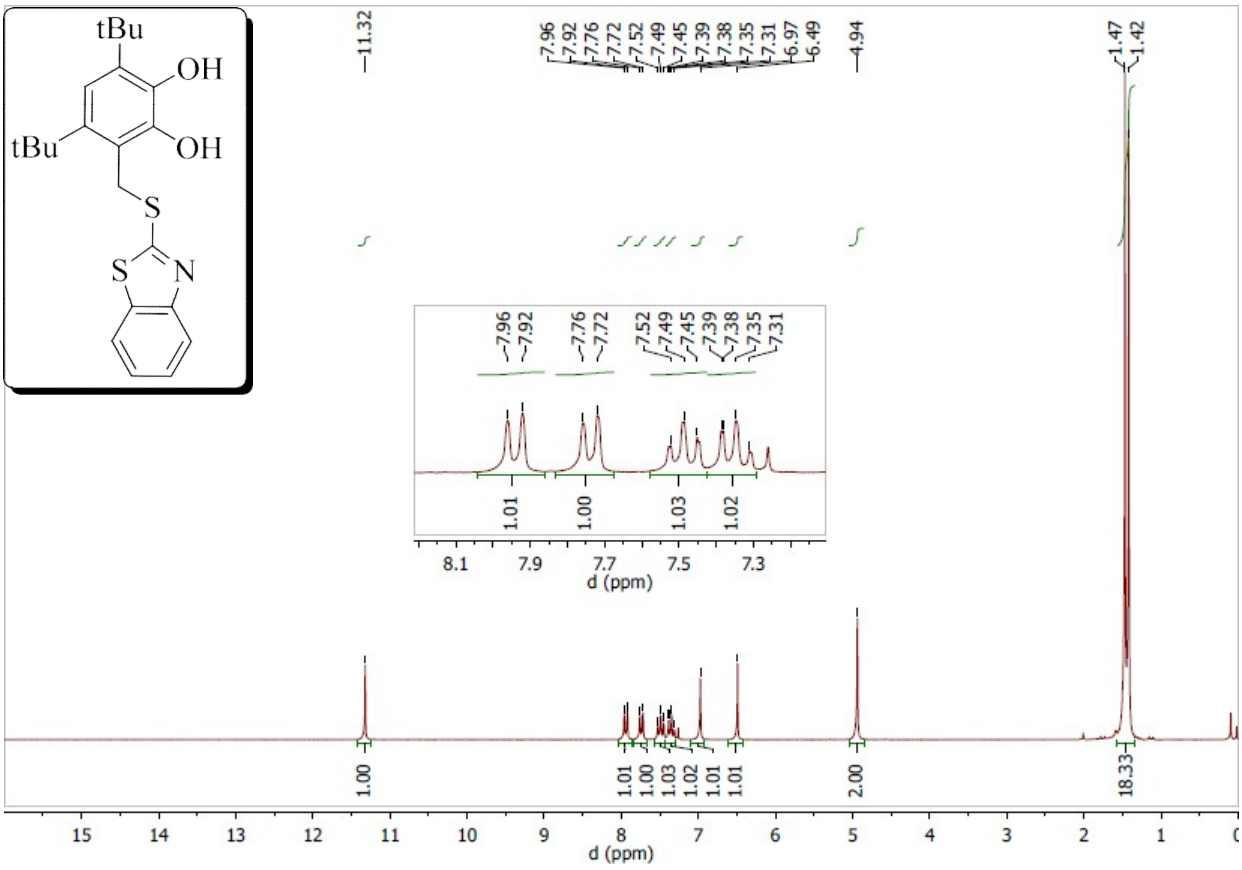

Figure S13. The ^{1}H NMR spectrum of **8** (200 MHz, $CDCl_3$).

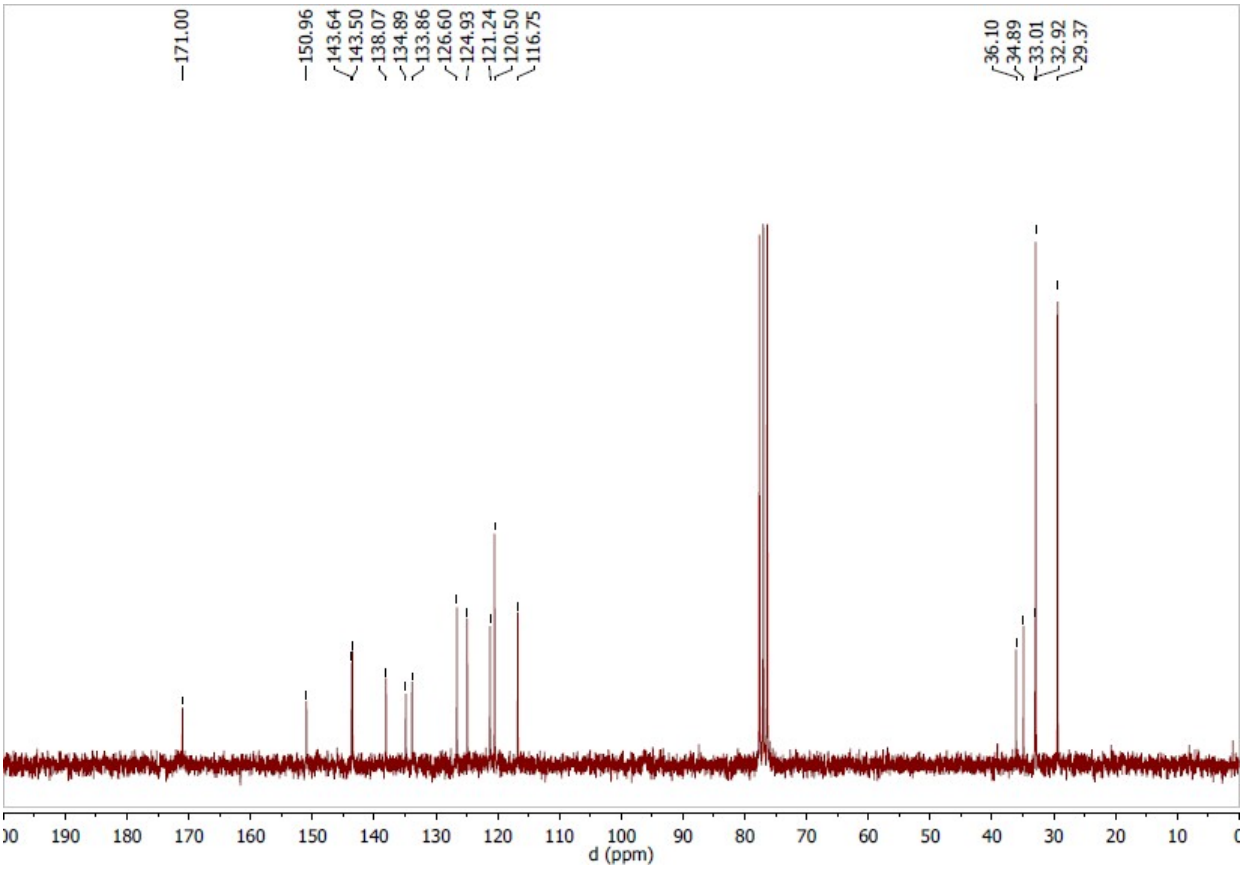

Figure S14. The $^{13}C\{^{1}H\}$ NMR spectrum of **8** (50 MHz, $CDCl_3$).

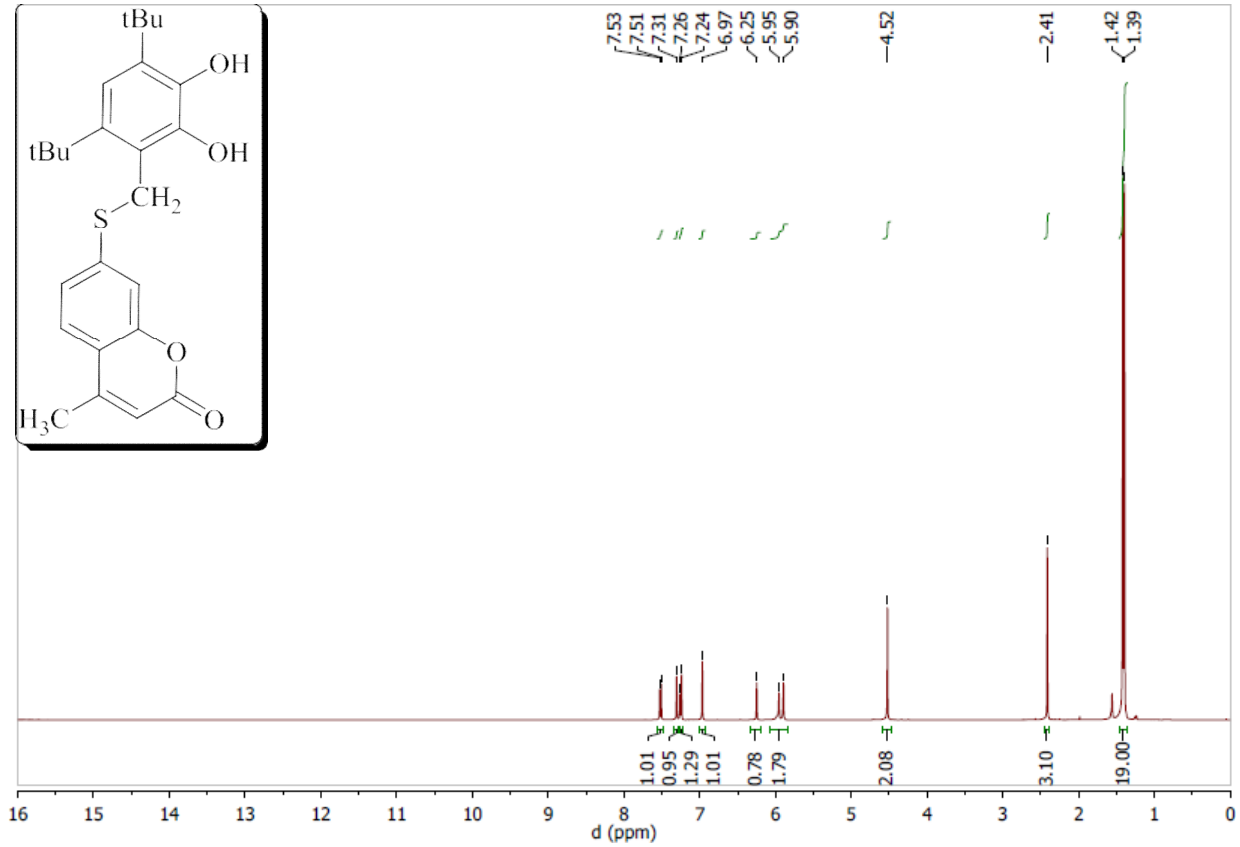

Figure S15. The ^{1}H NMR spectrum of **9** (400 MHz, $CDCl_3$).

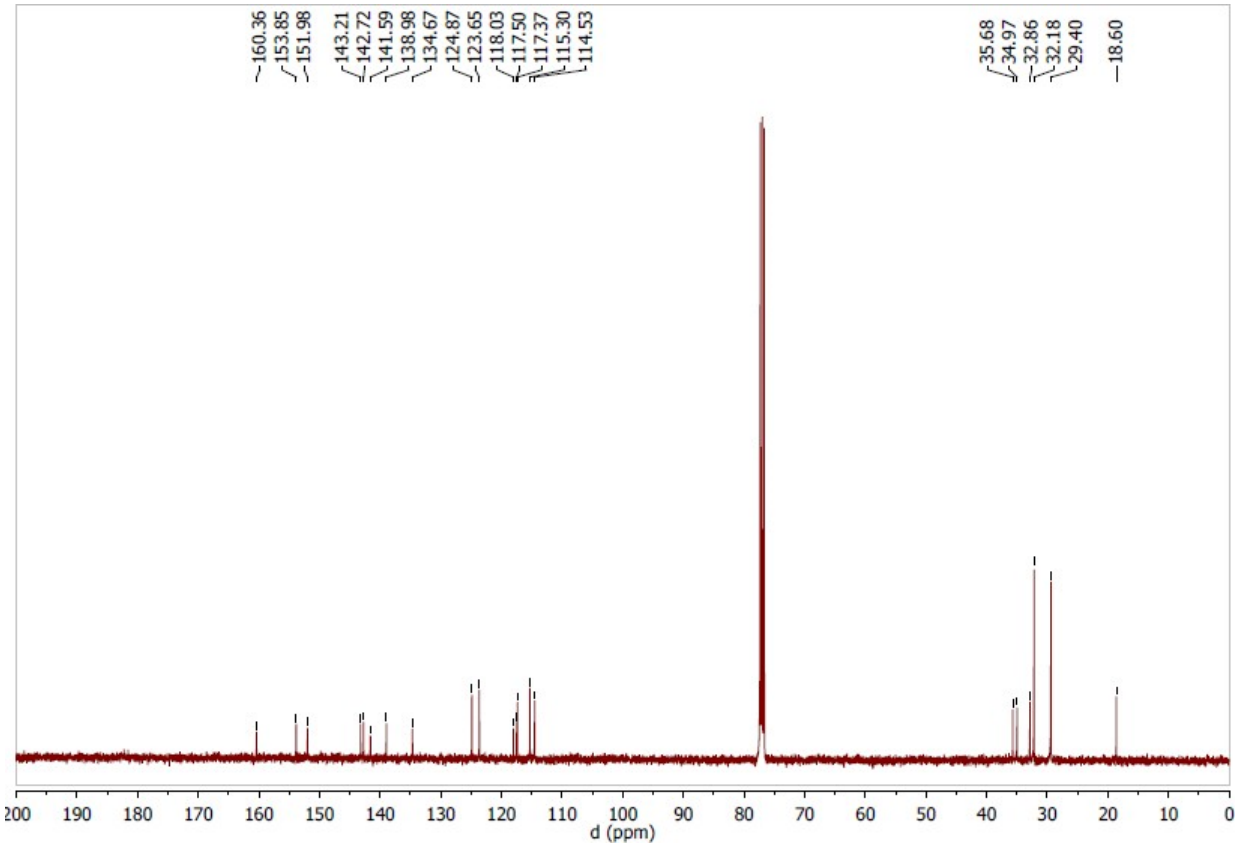

Figure S16. The $^{13}C\{^{1}H\}$ NMR spectrum of **9** (100 MHz, $CDCl_3$).

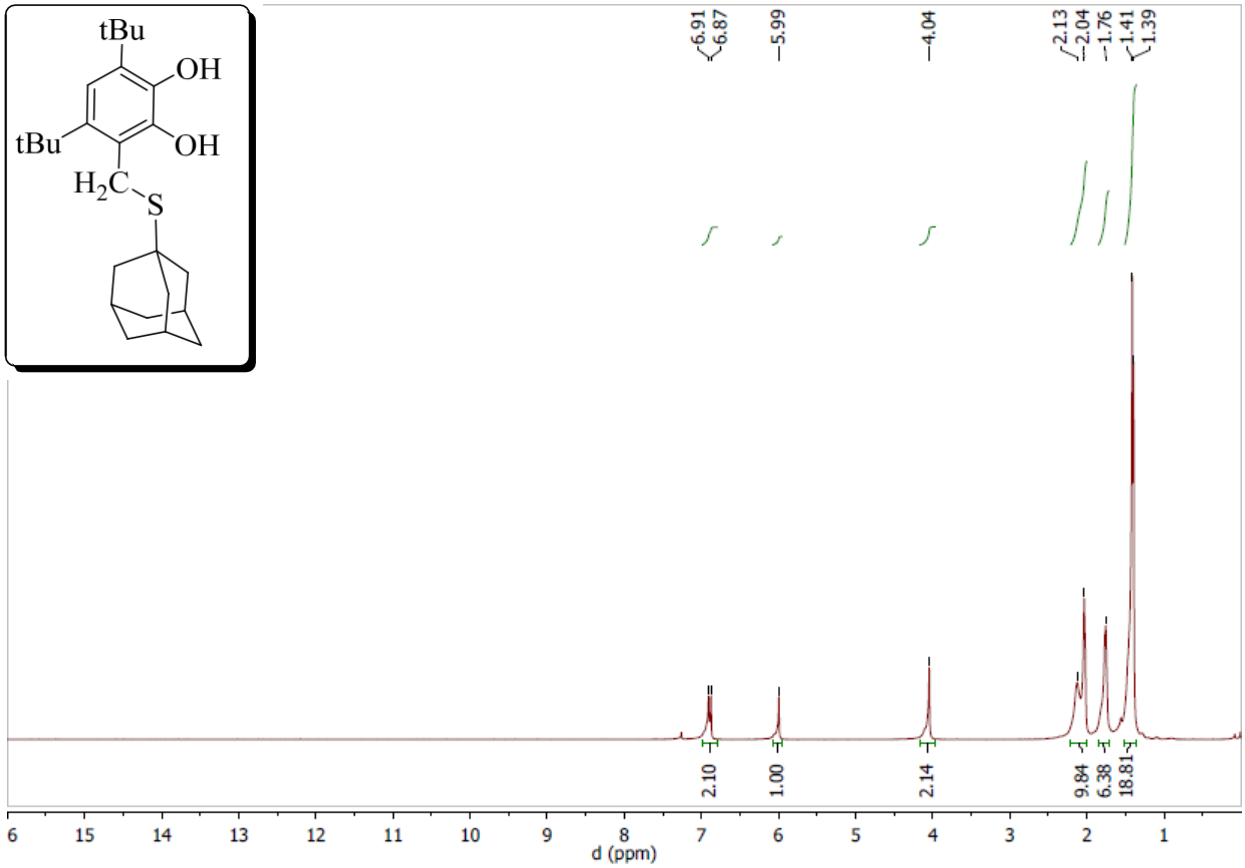

Figure S17. The ^{1}H NMR spectrum of **10** (200 MHz, $CDCl_3$).

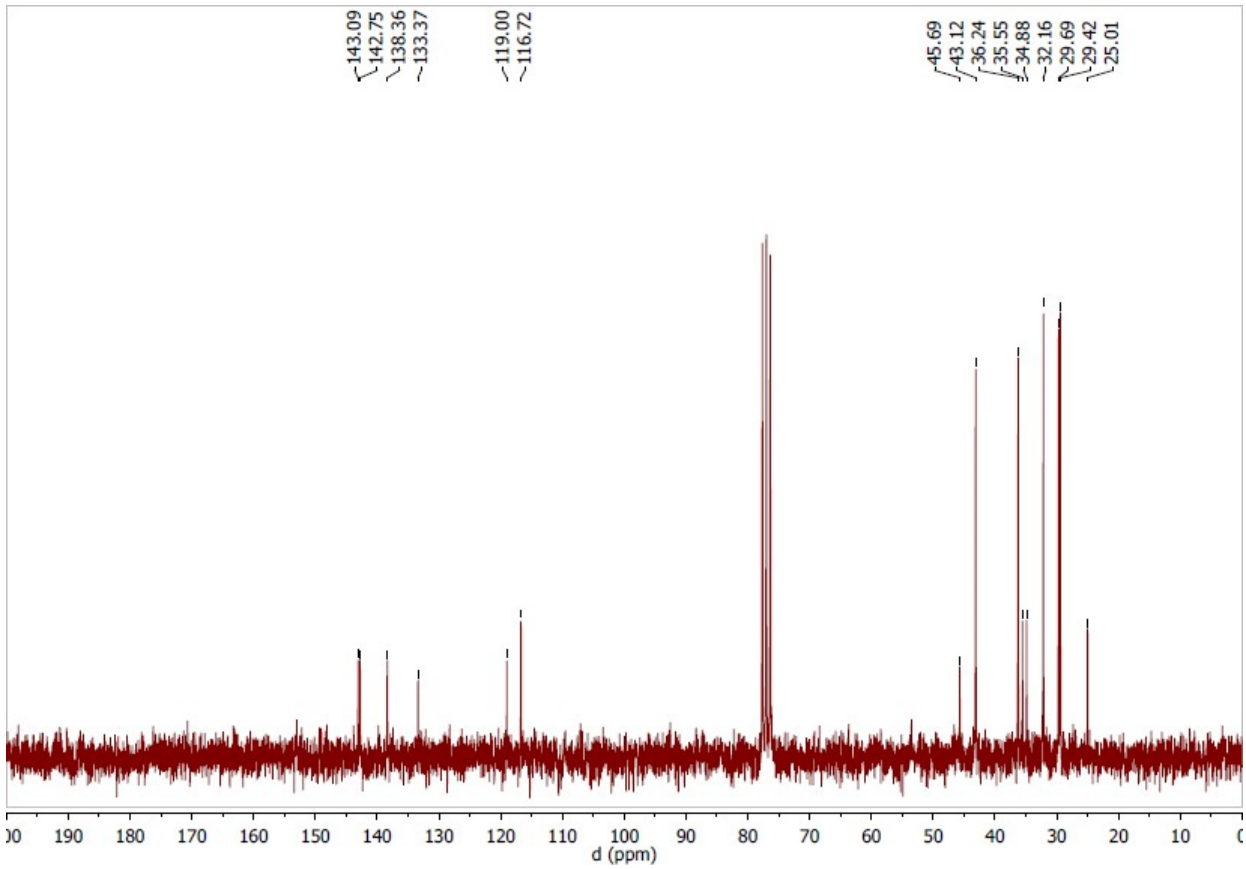

Figure S18. The $^{13}C\{^{1}H\}$ NMR spectrum of **10** (50 MHz, $CDCl_3$).

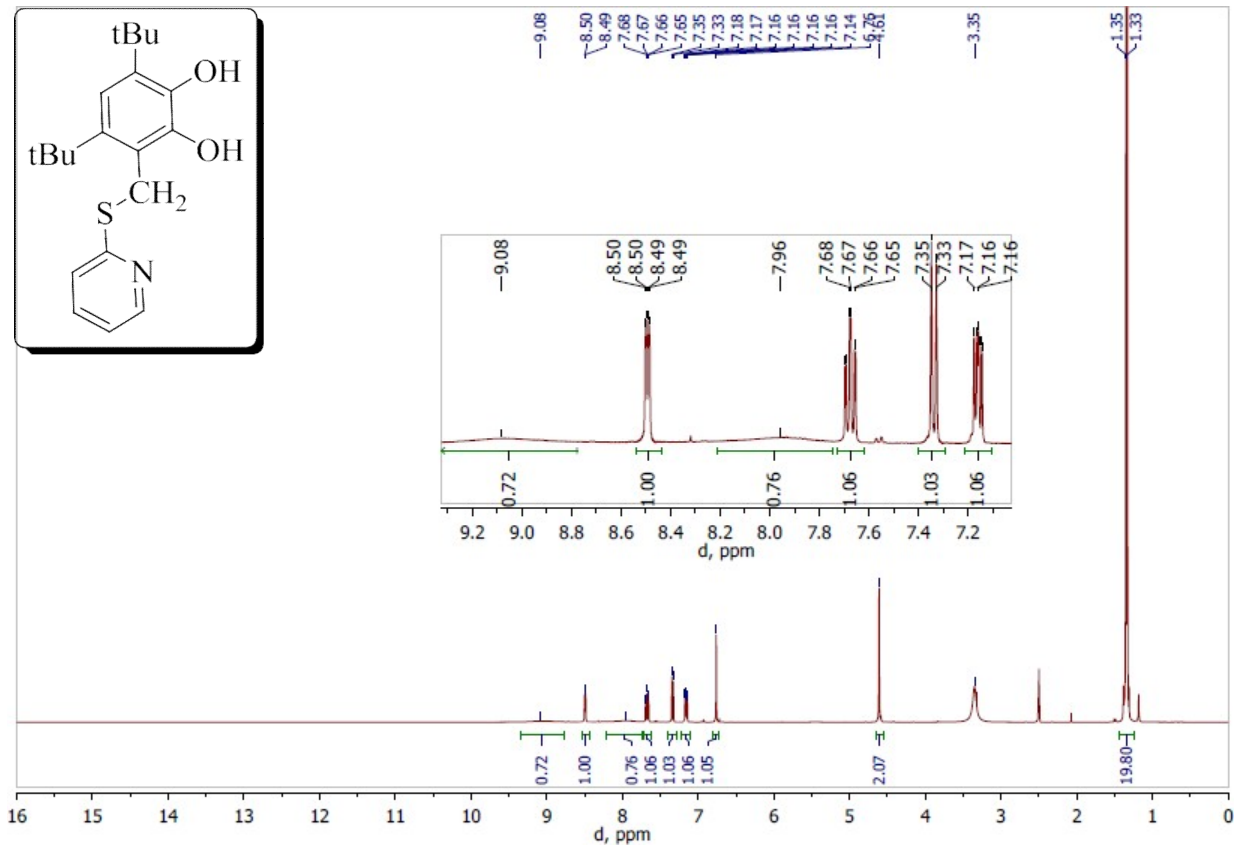

Figure S19. The ^{1}H NMR spectrum of **11** (400 MHz, DMSO-d_6).

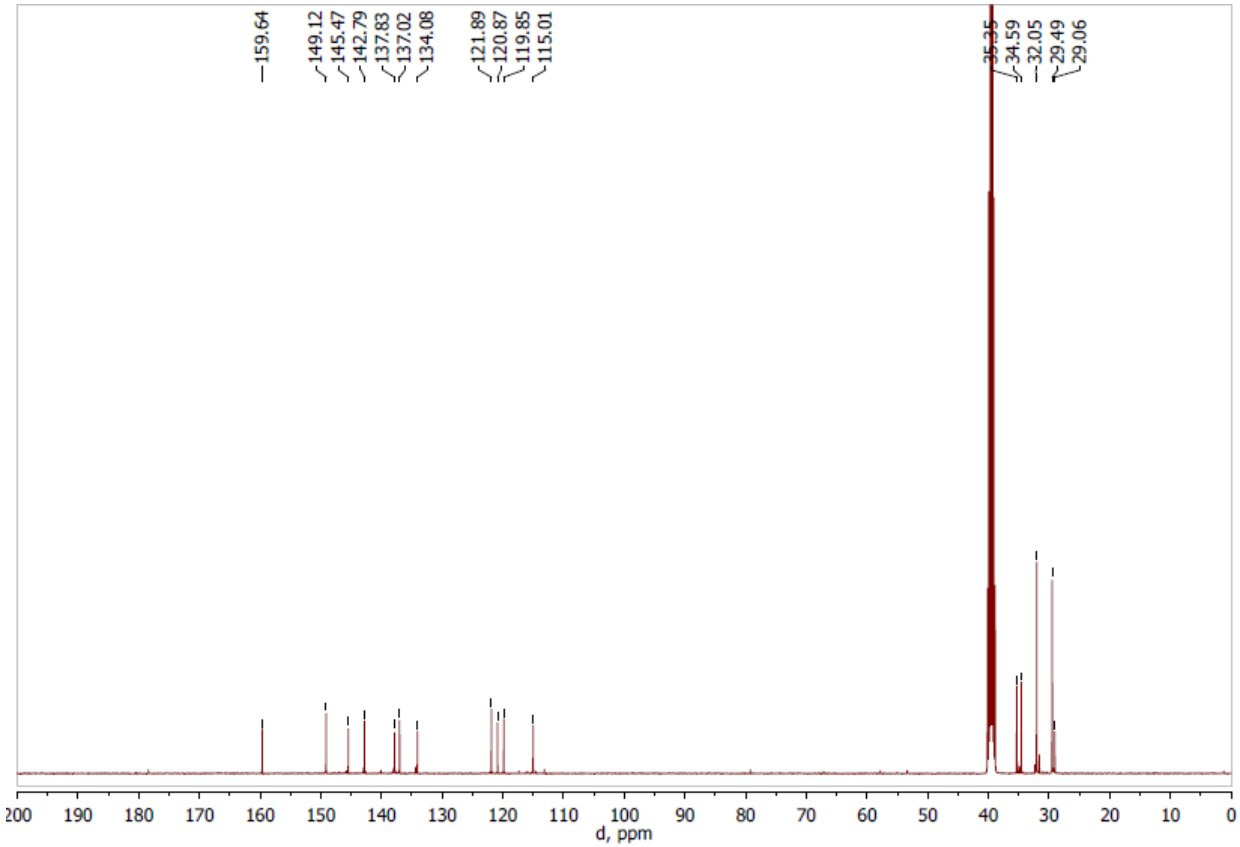

Figure S20. The ^{13}C{^{1}H} NMR spectrum of **11** (100 MHz, DMSO-d_6).

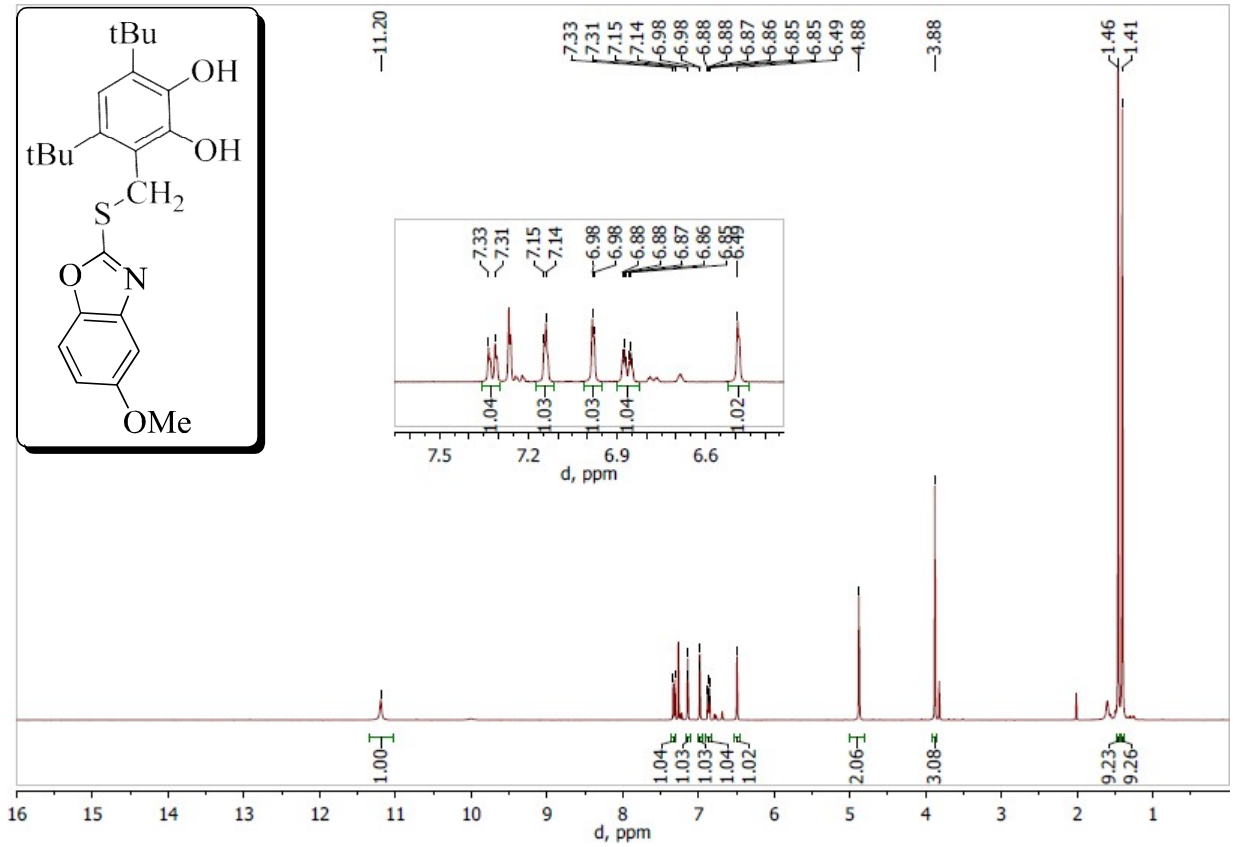

Figure S21. T he ^{1}H NMR spectrum of **12** (400 MHz, $CDCl_3$).

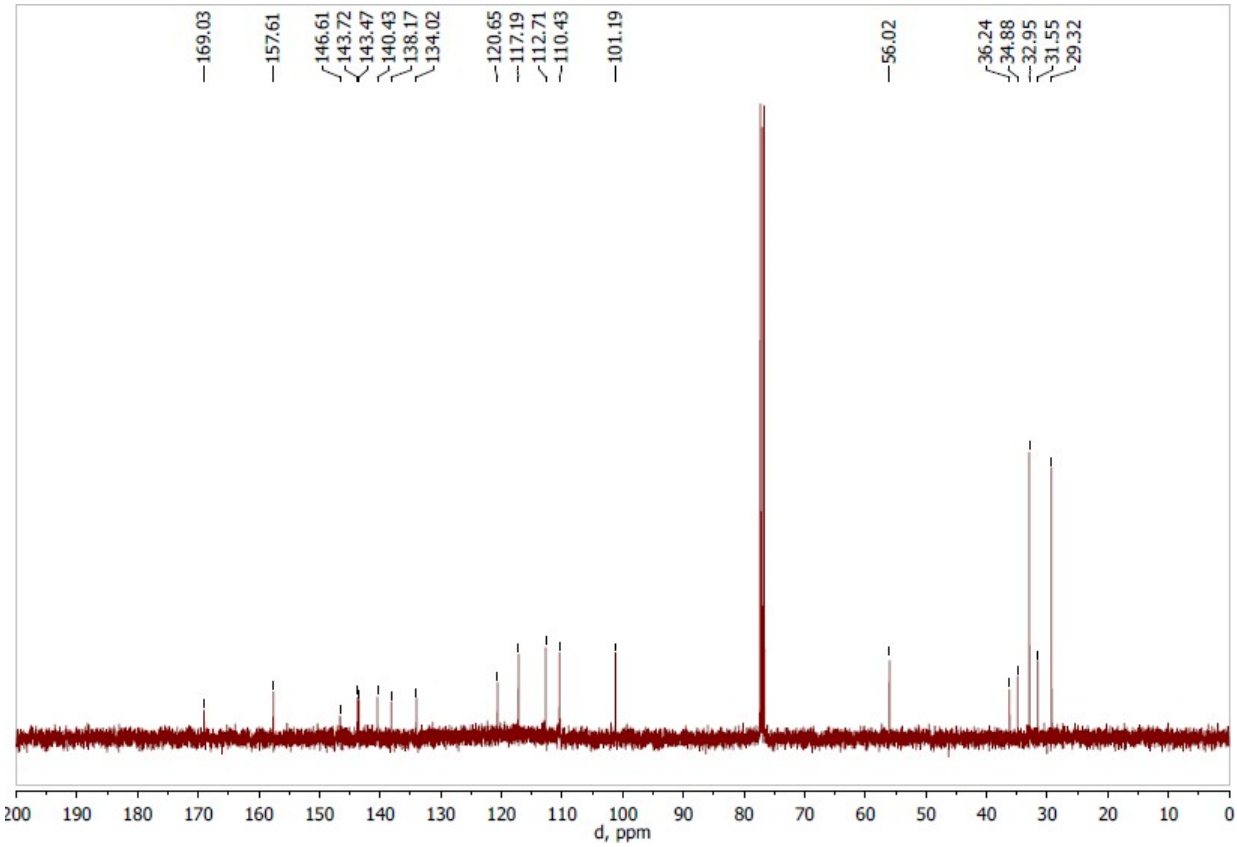

Figure S22. The $^{13}C\{^{1}H\}$ NMR spectrum of **12** (100 MHz, $CDCl_3$).

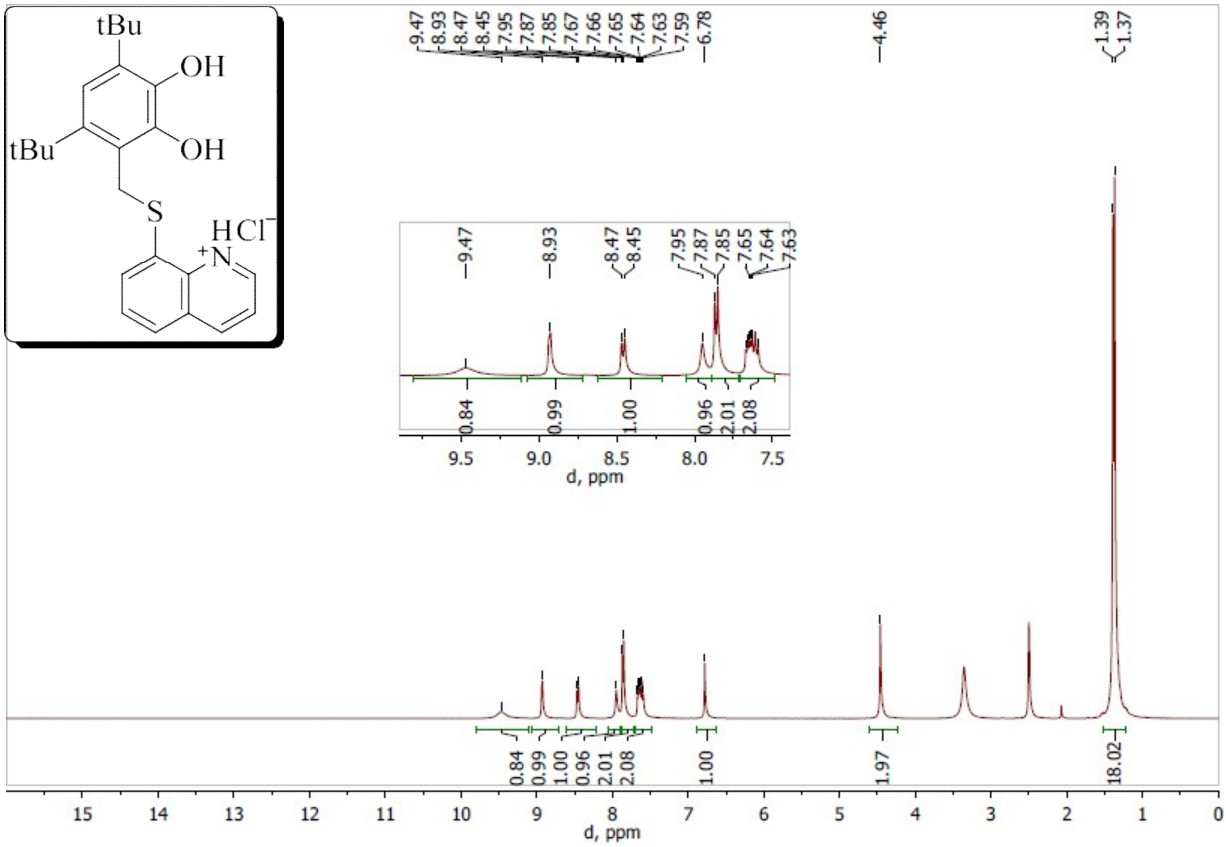

Figure S23. T he ^{1}H NM R spectrum of **13** (400 MHz, DMSO-d_6).

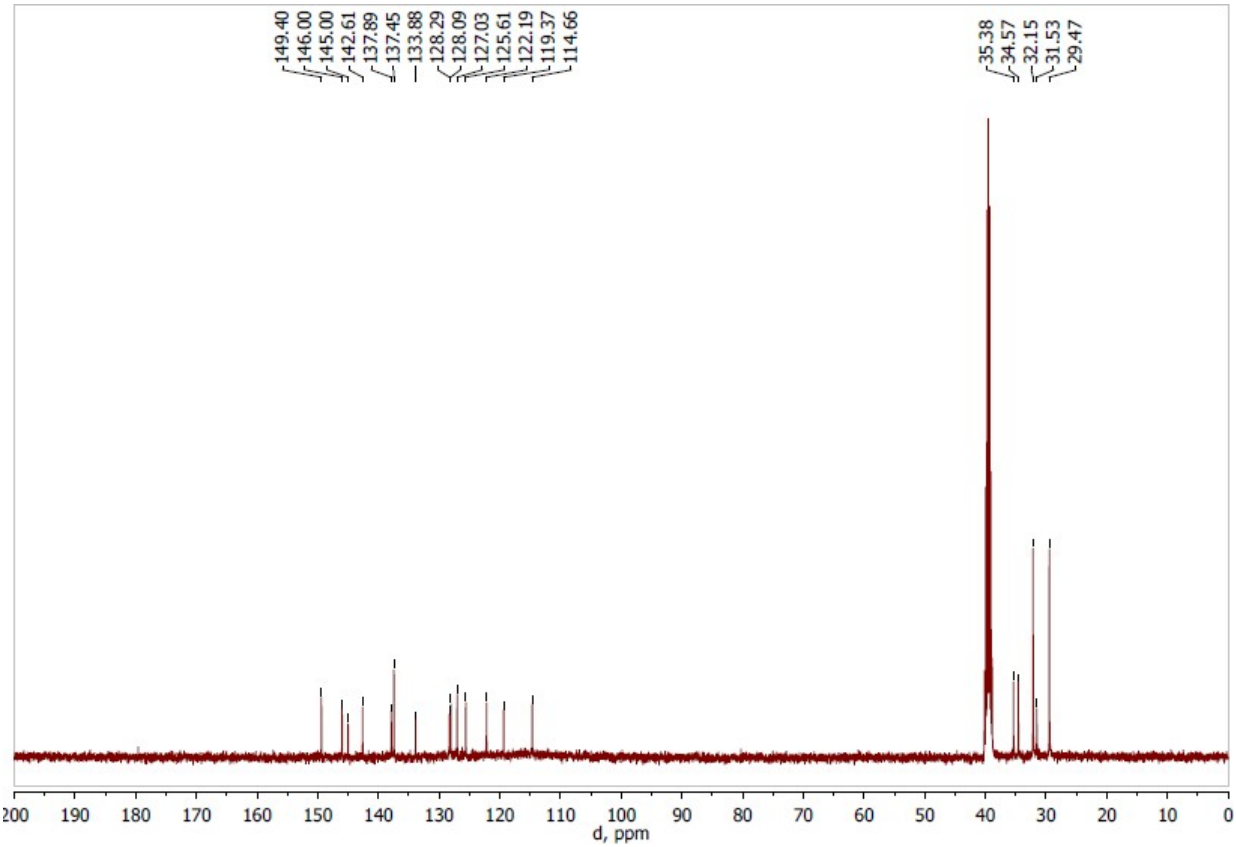

Figure S24. The ^{13}C{^{1}H} NMR spectrum of **13** (100 MHz, DMSO-d_6).

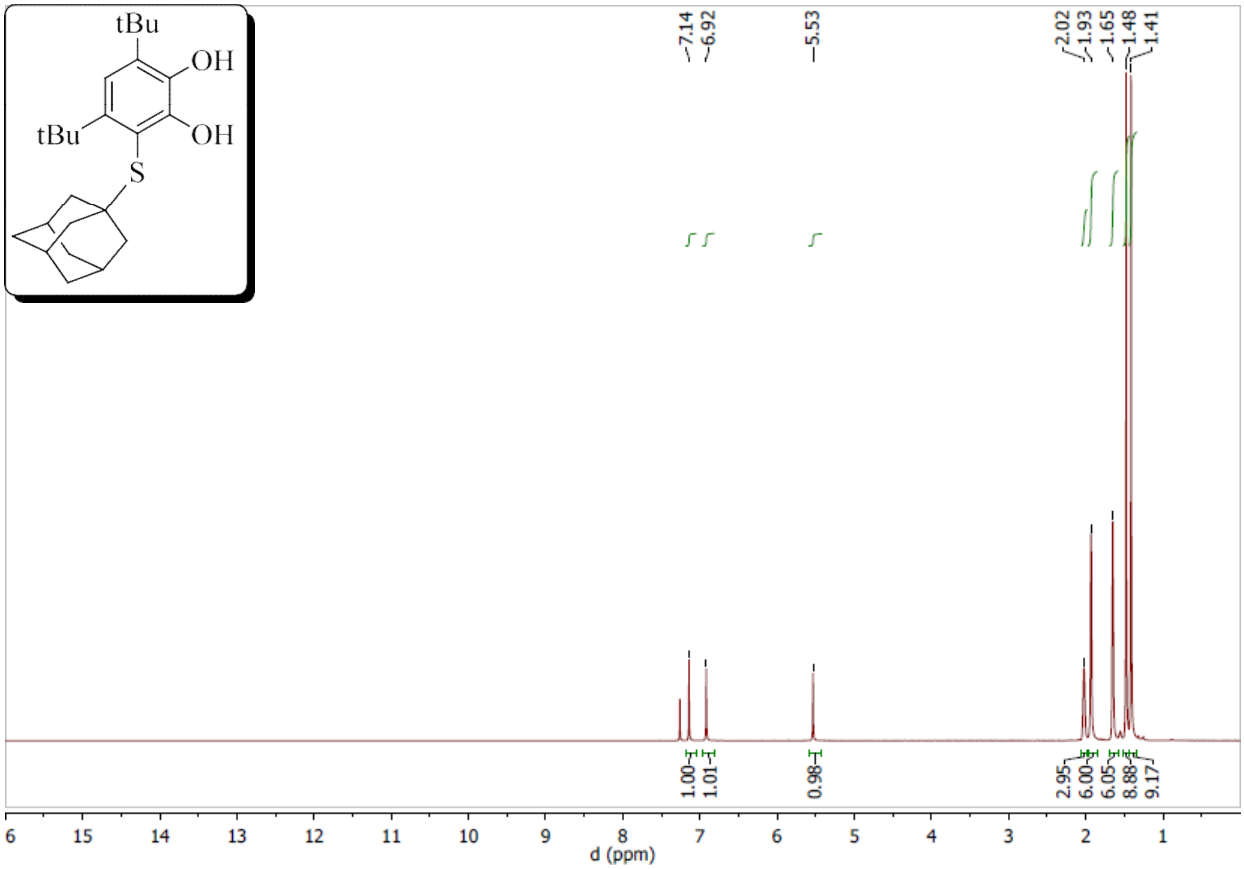

Figure S25. T he ^{1}H NMR spectrum of **14** (400 MHz, $CDCl_3$).

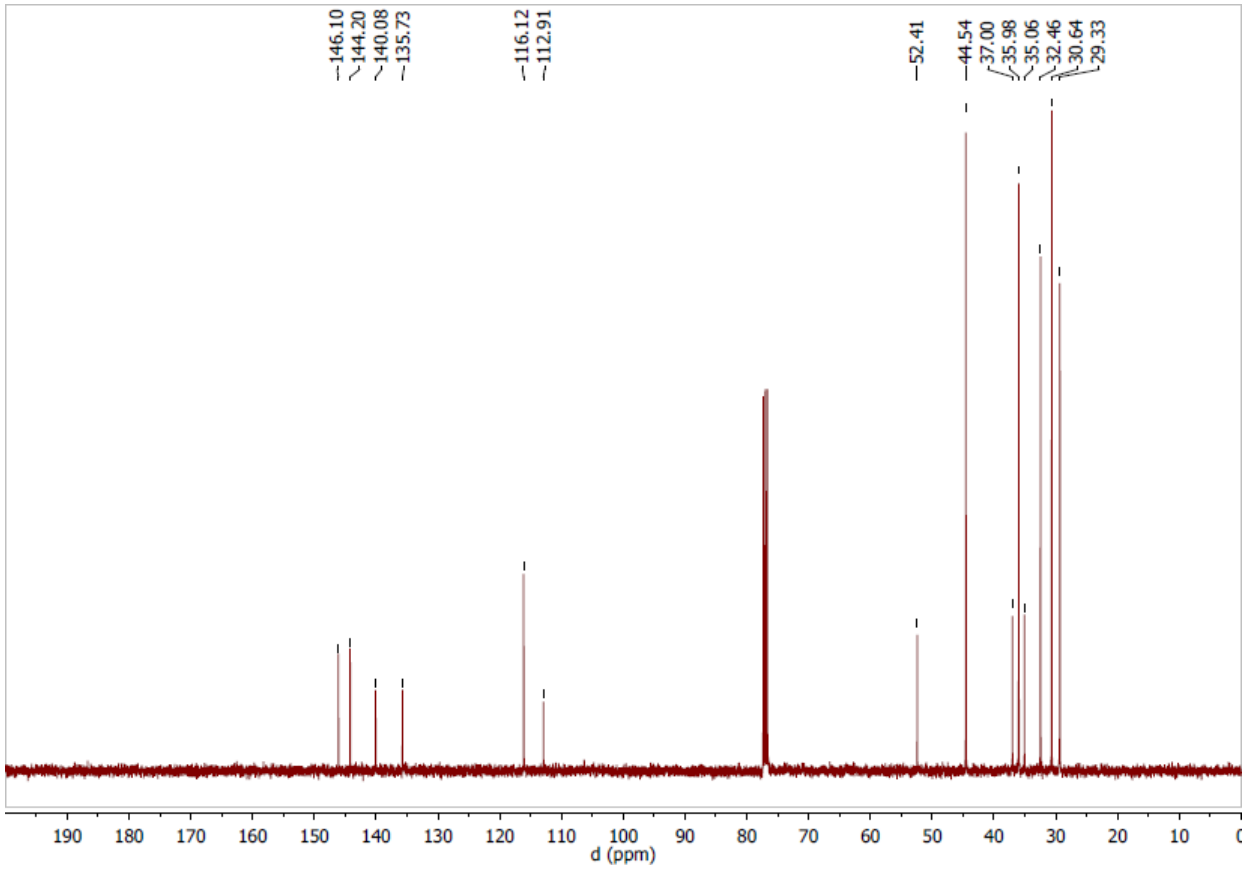

Figure S26. The ^{13}C{^{1}H} NMR spectrum of **14** (100 MHz, $CDCl_3$).

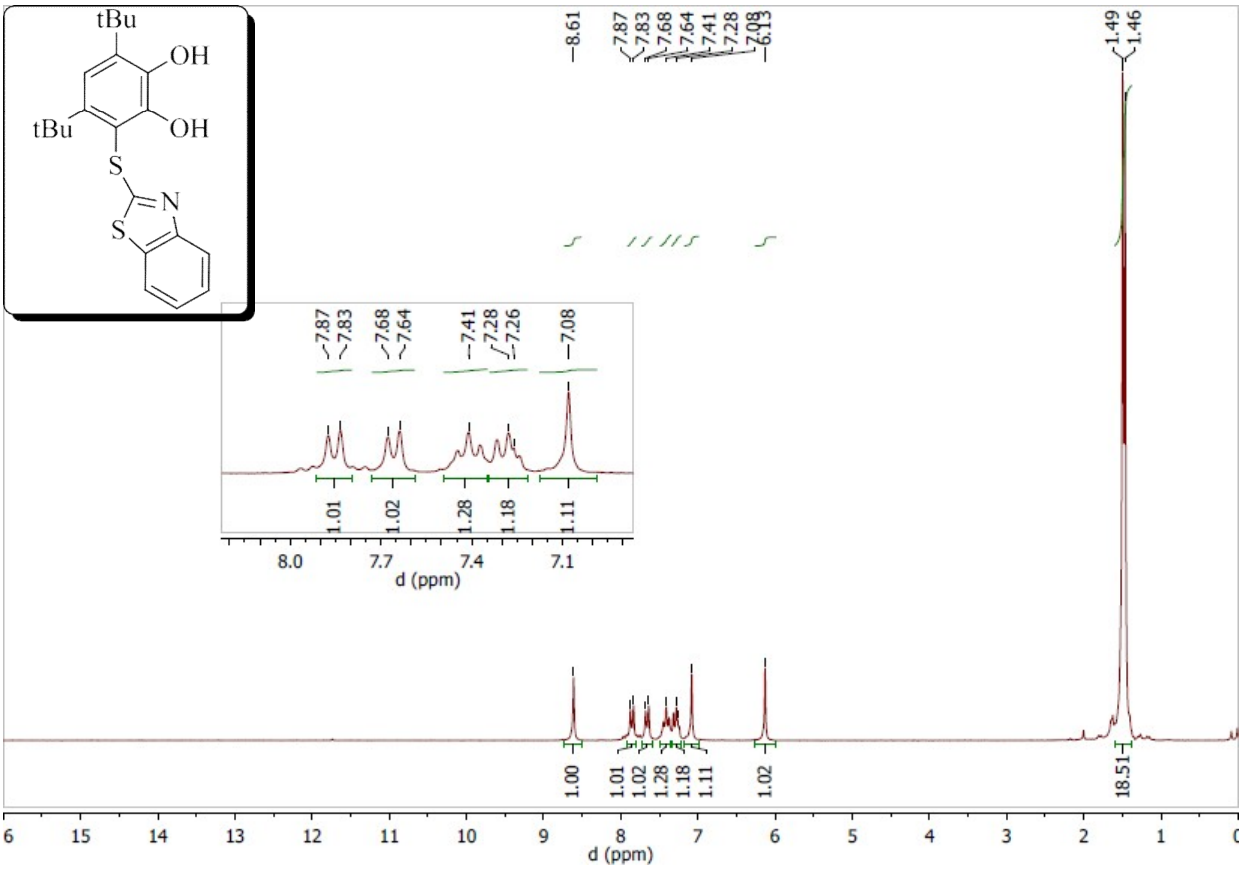

Figure S27. T he ^{1}H NMR spectrum of **15** (400 MHz, $CDCl_3$).

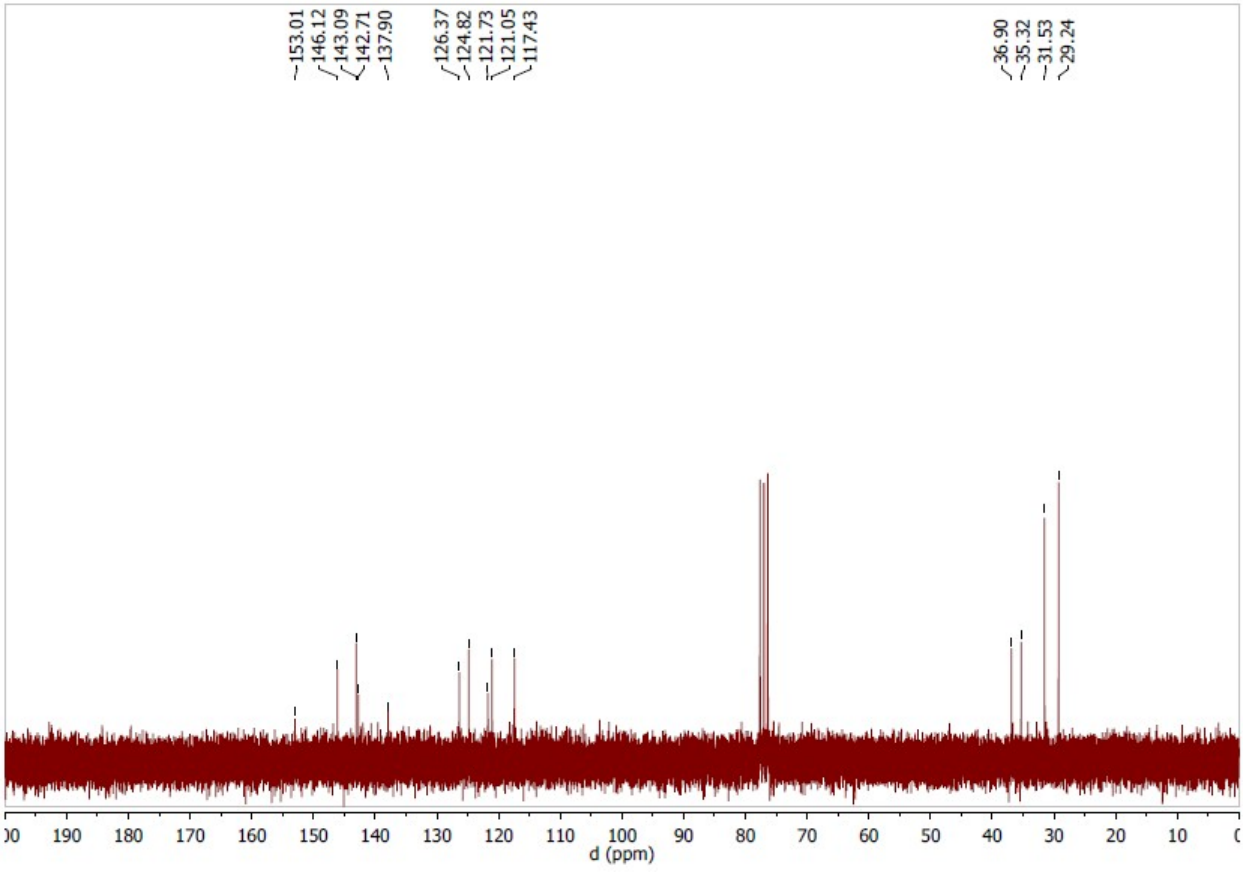

Figure S28. The ^{13}C{^{1}H} NMR spectrum of **15** (100 MHz, $CDCl_3$).

Table S1. Crystal data and structure refinement for **8** and **15**.

Compound	**8**	**15**
Empirical formula	$C_{22}H_{27}NO_2S_2$	$C_{21}H_{25}NO_2S_2$
Formula weight	401.56	387.54
Temperature, K	298(2)	298(2)
Wavelength, Å	0.71073	
Crystal system	Monoclinic	Triclinic
space group	P2(1)/n	P-1
Unit cell dimensions		
a, Å	9.3517(7)	9.5246(9)
b, Å	15.8237(11)	9.9168(11)
c, Å	15.0865(10)	11.0339(9)
alpha , deg.	90	88.784(8)
beta, deg.	106.800(2)	87.994(7)
gamma, deg.	90	82.011(9)
Volume, $Å^3$	2137.2(3)	1031.30(17)
Z	4	2
Calculated density, Mg/m^3	1.248	1.248
Absorption coefficient, mm^{-1}	0.265	0.273
F(000)	856	412
Crystal size, mm	0.33 x 0.17 x 0.12	0.36 x 0.24 x 0.15
Theta range for data collection, deg.	2.304 - 26.022	2.888 - 26.021
Limiting indices	$-11 \le h \le 11$ $-19 \le k \le 19$ $-18 \le l \le 18$	$-11 \le h \le 11$ $-12 \le k \le 12$ $-13 \le l \le 13$
Reflections collected / unique	28454 / 4210 [R(int) = 0.0477]	17741/4059 [R(int) = 0.1186]
Completeness to theta = 25.242, %	99.8	99.8
Absorption correction	Semi-empirical from equivalents	Analytical
Max. and min. transmission	0.9582 and 0.8453	0.964 and 0.927
Refinement method	Full-matrix least-squares on F^2	Full-matrix least-squares on F^2
Data / restraints / parameters	4210 / 0 / 258	4059 / 0 / 243
Goodness-of-fit on F^2	1.070	1.039
Final R indices [I>2sigma(I)]	R1 = 0.0468, wR2 = 0.1236	R1 = 0.0522, wR2 = 0.1237
R indices (all data)	R1 = 0.0625, wR2 = 0.1321	R1 = 0.0677, wR2 = 0.1354
Largest diff. peak and hole, $e \cdot Å^{-3}$	0.225 and -0.271	0.314 and -0.331